Magnetospheric Multiscale Satellite Observations of Parallel Electron Acceleration in Magnetic Field Reconnection by Fermi Reflection from Time Domain Structures

F. S. Mozer, O. A. Agapitov, A. Artemyev, J. L. Burch, R. E. Ergun, B. L. Giles, D. Mourenas, R. B. Torbert, T. D. Phan, and I. Vasko

Phys. Rev. Lett. **116**, 145101 — Published 5 April 2016

DOI: 10.1103/PhysRevLett.116.145101

Magnetospheric Multiscale Satellite observations of parallel electron acceleration in magnetic field reconnection by Fermi reflection from time domain structures

By F.S. Mozer[1], O.A. Agapitov[1,2], A. Artemyev[3,9], J.L. Burch[4], R.E. Ergun[5], B.L. Giles[6], D. Mourenas[7], R.B. Torbert[8], T. Phan[1], and I. Vasko[9]

1. Space Sciences Laboratory, University of California, Berkeley, California 94720, USA
2. Taras Shevchenko National University of Kyiv, Glushkova ave., 4, 03127, Kyiv, Ukraine
3. Institute of Geophysics and Planetary Physics, University of California, Los Angeles, California, USA
4. Southwest Research Institute, San Antonio, Texas, USA
5. LASP, University of Colorado, Boulder, Colorado, USA
6. NASA Goddard Space Flight Center, Greenbelt, Md. USA.
7. LPC2E/CNRS-University of Orleans, Orleans, France
8. University of New Hampshire, Durham, NH., USA
9. Space Research Institute, Russian Academy of Science, Moscow, Russia 117917

ABSTRACT

The same time domain structures (TDS) have been observed on two Magnetospheric Multiscale Satellites (MMS) near the Earth's dayside magnetopause. These TDS, traveling away from the X-line along the magnetic field at 4000 km/sec, accelerated field-aligned ~5 eV electrons to ~200 eV by a single Fermi reflection of the electrons by these overtaking barriers. Additionally, the TDS contained both positive and negative potentials so they were a mixture of electron holes and double layers. They evolve in ~10 km of space or 7 milliseconds of time and their spatial scale size is 10-20 km which is much larger than the electron gyroradius (<1 km) or the electron inertial length (4 km at the observation point, less nearer the X-line).

I. INTRODUCTION

Electron acceleration in space plasmas (the Earth's auroral zone, magnetosphere and magnetopause, and at other planets, the sun and other stars, etc.) is a persistent feature that is not well-understood and that has been poorly measured. The Magnetospheric Multiscale Satellites (MMS) were launched on March 12, 2015 [26] to measure, with unprecedented spatio-temporal detail, local acceleration processes as part of a broader study of magnetic field reconnection [34]. MMS consists of four closely spaced satellites (~10 km) equipped with high time resolution (~30 msec) measurements of electron distribution functions and higher time resolution (0.1 msec) measurements of electric and magnetic fields. MMS has flown through reconnection events at the dayside magnetopause to observe Time Domain Structures (TDS) that are reported in this paper to accelerate electrons from ~5 eV to ~200 eV by a single Fermi interaction of the charged particles reflected by the potential barrier of the overtaking TDS. Such a fast and strong acceleration process (corresponding to a factor of ~40 energy increase) may be one important new component in the chain of phenomena associated with reconnection and leading to global plasma heating [31,35]. Although, the absolute energy of the accelerated particles in this event is not very large, the acceleration factor of 40 is impressive and it could lead to greater accelerated energies for different plasma parameters. TDS are millisecond duration pulses of parallel electric field that move along the magnetic field line at thousands of km/sec. They may be

electrostatic or electromagnetic and they represent electron holes, double layers, or more complicated solitary waves. Because their potential structures are more complicated than the simple potential of an ideal electron hole or an ideal double layer, they are grouped into the generic category of TDS in this and earlier papers. TDS of one type or another have been theoretically studied in more than 250 articles dating back more than 50 years [1,2] and they have been found in the magnetosphere along auroral zone magnetic field lines on the S3-3 satellite [3,4], they were more thoroughly studied on later auroral missions [5,6], they have been seen in the magnetotail [7,8,9], the plasma sheet [10,11], the plasma sheet boundary layer [12], at shocks [13,14], at magnetic field reconnection sites [15,16,17,18,19], in the solar wind [20,21,22], and at Saturn [23]. Interest in their properties and their ability to accelerate electrons to hundreds of keV has been enhanced by observations of huge fluxes of TDS on the Van Allen Probes in the Earth's radiation belts [24, 25].

II. OBSERVATIONS

Figure 1 presents 150 msec of high-pass-filtered parallel electric field measurements made on the four MMS spacecraft. MMS4 and MMS1 saw seven correlated spiky parallel electric fields (the TDS) while MMS2 may have seen the last 3 of these spikes and MMS3 saw nothing. The parallel and perpendicular separations of the spacecraft are given in Table I. MMS1 and MMS4, separated by 9.3 kilometers perpendicular to the magnetic field saw the TDS pairs while the other spacecraft, separated by 22-27 km perpendicular to the magnetic field, may not have. This suggests that the perpendicular scale size of these TDS was 10-20 km, i.e. much larger than the thermal electron gyroradius (<1 km) or the electron inertial length (4 km at the observation site, less nearer the X-line).

The electric fields of the second matching pair of TDS observed on the two spacecraft are illustrated with higher time resolution in the top panel of Figure 2, with those observed on MMS4 delayed by 7.9 msec. Because their parallel separation was 29.2 km and their temporal separation was 7.9 msec, their speed along the magnetic field line was about 4000 km/sec. It is noted that the MMS4 and MMS1 fields differed, with the positive electric field in the earlier measurement (on MMS4) being about three times larger than in the later measurement. This suggests that the structures varied spatially or temporally on scales of several electron gyroradii or gyroperiods. The bottom panel of Figure 2 is the electric potential obtained by integrating the data in the top panel. The peak negative potential was about -20 volts with an estimated uncertainty of 30% related to the variation of the response as a function of frequency of the on-axis electric field antenna (that observed most of the parallel electric field).

The TDS all had positive and negative potential parts. The positive potential parts of the TDS that overtake an electron have little net effect on the electron because the fields in such potentials slightly decelerate then re-accelerate the electron as the TDS passes by. However, the electric fields in the negative potential parts of a TDS that overtakes an electron will accelerate the electron away from the TDS in a process that looks like a moving wall (the parallel potential) reflecting the slower electrons by the electrostatic Fermi interaction [27,28]. This mechanism will be discussed following presentation of the electron data. A similar acceleration mechanism has been suggested for generation of field-aligned electron fluxes in the Earth's outer radiation belt [29].

The components of the magnetic field in GSE coordinates, measured at the time of the TDS (the vertical dashed line in the figure), are shown in panels 3(a)-3(c) of Figure 3. The change of the z-component of the field signified the magnetopause crossing and the observations were located approximately in the magnetospheric separatrix, as illustrated in figure 3(d). Previous observations demonstrate that TDSs often propagate away from the reconnection region along the magnetic separatrix [30] and such TDS have been discussed as being associated with electron acceleration during reconnection [31].

The upper panel of Figure 4 presents 400 msec of 131 eV electron energy flux measured at three pitch angles during the time interval when the TDS passed over spacecraft 1. The TDS moved opposite to the magnetic field direction and the 174 degree electron flux (which was moving in that direction) decreased at the time of the TDS, suggesting that the 131 eV flux was influenced by the TDS. A possibility is that the TDS overtook low energy electrons and accelerated them via the Fermi mechanism associated with the electrons bouncing off a moving barrier only once. If this happened, the 174 degree electrons with velocities higher than the TDS speed observed before the TDS crossed the spacecraft, were accelerated by the TDS while the same energy electrons measured after the TDS crossing were not. Thus, the ratio of electron fluxes before and after the TDS crossing can provide information on the TDS interaction, as is illustrated in the bottom panel of Figure 4. The vertical dashed line in this panel is the energy of an electron moving at a speed of 4000 km/sec. The before-to-after electron flux ratio is about 0.8-1.0 for particle velocities around the TDS speed, but it becomes significantly larger than one (reaching ~ 1.6) for velocities higher than the TDS speed. Thus, it appears that electrons with field-aligned velocities less than that of the TDS were accelerated to 200 eV or greater by the overtaking TDS. This conclusion is supported by the before-and-after phase space densities presented in Figure 5 in which, for 174 degree electrons (the upper panel), <100 eV electrons were apparently accelerated to >100 eV by the TDS passage.

After TDS passage in Figure 5 (when the observed electrons have not encountered the TDS) the spectrum was flat. Before TDS passage, the accelerated electrons produced a positive slope in the phase space density. This unstable situation may result in further wave-particle interactions that remove the positive slope and affect the energies of the electrons that created it. The plateau, at energies comparable to the energy associated with the TDS speed, may correspond to the relaxed beam that generated the observed TDS.

III. DISCUSSION

A quantitative estimate of the Fermi acceleration is obtained by defining the parallel speeds in the satellite frame of reference of the TDS as v_{tds} and the electron as v_e. In the TDS frame, the TDS speed is 0 and the electron speed is $(v_e - v_{tds})$. After elastic collision with the TDS, the electron velocity changes sign and becomes $(v_{tds} - v_e)$. Thus, in the satellite frame, the final electron speed is $(2v_{tds} - v_e)$ and its energy is $\frac{1}{2}m(2v_{tds} - v_e)^2$. A plot of the electron final energy as a function of its initial energy is given in Figure 6(a) for a 4000 km/sec barrier,

A limit that prevents low energy electrons from being accelerated to the ~180 eV maximum energy for a TDS speed of 4000 km/sec (Figure 6a) is that the potential barrier must be large

enough to reflect an incident electron. Thus, $\frac{1}{2}m(v_{tds} - v_e)^2$ must be less than the (negative) potential of the TDS. A plot of the minimum potential barrier as a function of the initial electron energy is given in Figure 6b. In the case of interest, the potential barrier was about 20 volts, so incident electrons with energies less than about 5 eV were not reflected by the barrier. Thus, the most energetic Fermi accelerated electrons would have an energy of about 125 eV if the TDS speed was 4000 km/sec.

There are two discrepancies between the analysis thus far and the data. The first is that the measured upper bound on the accelerated electron energy of ~250 eV (lower panel of Figure 4) is much greater than the 125 eV maximum energy obtained for Fermi acceleration by a 4000 km/sec TDS (Figure 6a). The second discrepancy is that the energetic electrons disappeared (upper panel of Figure 4) about 150 milliseconds before the TDS arrived at the spacecraft (Figure 1). Both of these discrepancies are resolved if the TDS earlier had a greater speed, as the following estimate shows. Suppose that the TDS had a speed of 6000 km/sec when it was a distance, d, from the spacecraft and that its speed decreased linearly to 4000 km/sec during the time, T, that it moved the distance, d, to the spacecraft. Further, suppose that the ~200 eV electrons were accelerated at the distance, d, and arrived at the spacecraft after traveling (T-0.15) seconds. These two assumptions produce two equations in two unknowns, d and T, whose values are d = 1800 km and T = 0.37 seconds. Thus, the ~200 eV electron acceleration occurred a fraction of a second before they crossed the spacecraft and at a distance of 10-20 ion inertial lengths upstream. In this way, the data provide additional evidence for the decay of the TDS as they moved along the magnetic field away from the X-line.

It is interesting to consider what may happen to an electron after undergoing the one-time Fermi acceleration. As shown in Figure 5(a), an incident 40 eV electron is accelerated to 57 eV by this interaction. As this accelerated electron moves into the converging magnetic field, its parallel velocity is converted to perpendicular velocity by conservation of the first adiabatic invariant. If the magnetic field converges sufficiently and the TDS survives over the convergence distance, the parallel speed of the electron of interest will slow to the speed of the TDS and it will undergo a further Fermi acceleration. In this way, the electron can move into the converging magnetic field at a roughly constant parallel velocity as its perpendicular energy increases due to multiple Fermi interactions in what amounts to a Landau resonance interaction between the electron and the TDS. There is no evidence, yet, whether a process like this is at work in reconnection events. However, in the outer Van Allen radiation belts this process has been shown to accelerate thermal (~100 eV) electrons to tens of keV [32] and even hundreds of keV [33].

ACKNOWLEDGEMENTS

The authors thank V. Krasnoselskikh for several useful comments and suggestions. We are deeply indebted to the entire MMS team that built such wonderful instruments and an outstanding program. The work of FSM and TP was supported by NASA grant NNX08AO83G. JLB, RBT and BLG were supported by NASA Contract NNG04EB99C at SwRI. The work of OVA and FSM was also supported under JHU/APL Contract No. 922613 (RBSP-EFW). AVA is grateful to the Dmitry Zimin Dynasty Foundation for support. The work of IYV was supported by the Presidental grant MK-7757.2016.2.

REFERENCES

1. A.S. Volokitin and V.V. Krasnoselskikh, *Sov. J. Plasma Physics*, 8(4), 454,(1982)

2. F.S. Mozer, O.V. Agapitov, A. Artemyev, J.F. Drake, V. Krasnoselskikh, S. Lefosne, and I. Vasko, *Geophys. Res. Lett.*, 10.1002/2015GL063946 (2015)

3. F.S. Mozer, C.W. Carlson, M.K. Hudson, R.B. Torbert, B. Parady, J. Yatteau and M.C. Kelley, *Phys. Rev. Lett.*, *38*, 292 (1977)

4. M.A. Temerin, K. Cerny, W. Lotko, and F.S. Mozer, *Phys. Rev. Lett.*, *48*, 1175 (1982)

5. R.E. Ergun et al, *Geophys. Res. Lett.*, *25*, 2041–2044, DOI:10.1029/98GL00636 (1998)

6. R.E. Ergun, Y.-J. Su, L. Andersson, C. W. Carlson, J. P. McFadden, F. S. Mozer, D. L. Newman, M. V. Goldman, and R. J. Strangeway, *Phys. Rev. Lett.*, *87 (4)*, 045003, DOI:10.1103/PhysRevLett.87.045003 (2001)

7. H. Matsumoto, H. Kojima, T. Miyatake, Y. Omura, M. Okada, I. Nagano, and M. Tsutsui, *Geophys. Res. Lett.*, *21*, 2915–2918, DOI:10.1029/94GL01284 (1994)

8. J.R. Franz, P.M. Kintner, J.S. Pickett, *Geophys. Res. Lett.*, Volume 25, Issue 8, p. 1277-1280 (1998)

9. T. Streed, C. Cattell, F.S. Mozer, S. Kokubun, and K. Tsuruda, *J. Geophys. Res.*, 106 (2001)

10. R.E. Ergun et al, *Phys. Rev. Lett.*, *102 (15)*, 155002, DOI:10.1103/PhysRevLett.102.155002 (2009)

11. X. Deng, M. Ashour-Abdalla, M. Zhou, R. Walker, M. El-Alaoui, V. Angelopoulos, R.E. Ergun, and D. Schriver, *J. Geophys. Res.*, 115, A09, 225, DOI:10.1029/2009JA015107(2010)

12. G.S. Lakhina, D.A. Gurnett, N. Cornilleau-Wehrlin, A.N. Fazakerley, I. Dandouras, and E. Lucek, Modern Challenges in Nonlinear Plasma Physics: A Festchrift Honoring the Career of K Papadopoulos, AIP Conference Proceedings 1320, American Institute of Physics, Melville, NY. (2010)

13. S.D. Bale, P.J. Kellogg, D.E. Larsen, R.P. Lin, K. Goetz, and R.P. Lepping, *Geophys. Res. Lett.*, *25*, 2929–2932, DOI:10.1029/98GL02111, (1998)

14. C. Cattell, C. Neiman, J. Dombeck, J. Crumley, J. Wygant, C. A. Kletzing, W. K. Peterson, F. S. Mozer, and M. Andre, *Science*, *299*, 383-6 (2003)

15. C. Cattell, C., J. Crumley, J. Dombeck, J. Wygant, F.S. Mozer, *Geophys. Res. Lett.*, *29*, 9-1 (2002)

16. F.S. Mozer and P.L. Pritchett *Geophys. Res. Lett.*, *36*, L07102, DOI:10.1029/2009GL037463, (2009)

17. F.S. Mozer and P. L. Pritchett, *J. Geophys. Res.*, DOI:10.1029/2009JA014718 (2009)

18. Y.V. Khotyaintsev, A. Vaivads, M. Andre, M. Fujimoto, A. Retino, and C. J. Owen, *Phys. Rev. Lett.*, *105(16)*, 165002, DOI:10.1103/PhysRevLett.105.165002 (2010)

19. S.Y. Li, Y. Omura, B. Lembege, X.H. Deng, H. Kojima, Y. Saito, and S.F. Zhang, *J. Geophys. Res., 119,*doi:10.1002/2013JA018920 (2014)

20. S.D. Bale, D. Burgess, P. J. Kellogg, et al, *Geophys Lett*, 11, *109* (1996)

21. D.M. Malaspina, D.L. Newman, L.B.III Wilson, K. Goetz, P.J. Kellogg, and K. Kersten, *J. Geophys. Res.*, 118 (2013)

22. J.D. Williams, L.-J. Chen, W.S. Kurth, D.A. Gurnett, M.K. Dougherty and A.M. Rymer, *Geophys. Rev. Lett., 32,* L17103, doi:10.1029/2005GL23079 (2005)

23. J.D. Williams, L.-J. Chen, W.S. Kurth, and D.A. Gurnett, *Geophys. Res. Lett., 33,* L06103, doi:10.1029/2005GL024532 (2006)

24. F.S. Mozer, S.D. Bale, J.W. Bonnell, C.C. Chaston, I. Roth, and J. Wygant, *Phys. Rev. Lett., 111* (2013)

25. F.S. Mozer, O.V. Agapitov, V. Krasnoselskikh, S. Lejosne, G.□D. Reeves, and I. Roth (2014), *Phys. Rev. Lett.*, *113*, 035001 (2014)

26. J.L. Burch, T.E. Moore, R.B. Torbert, and B.L. Giles, *Spa. Sci. Rev*., DOI 10.1007/s11214-015-0164-9 (2015)

27. E. Fermi, *Phys. Rev.*, 75, 1169 (1949).

28. D.A. Bryant, A.S. Cook, Z.S. Wang, U. de Angelis, C.H. Perry, *J. Geophys, Res.*, 96, 13829 (1991)

29. I. Y. Vasko, O.V. Agapitov, F.S. Mozer, A.V. Artemyev, *J. Geophys, Res.*, 120, 8616 (2015)

30. H. Viberg, Y.V.Khotyaintsev, A. Vaivads, M. André, J.S.Pickett, *Geophys. Res. Lett.*, Volume 40, Issue 6, pp. 1032-1037, (2013)

31. J. Egedal, W. Daughton, A. Le and A. L. Borg, *Phys. Plasmas* 22, 101208 (2015)

32. A. Artemyev, O.V. Agapitov, F.S. Mozer and V. Krasnoselskikh, *Geoph. Res. Lett.*, DOI: 10.1002/2014GL061248 (2014)

33. F.S. Mozer, A. Artemyev, O.V. Agapitov, D. Mourenas, and I. Vasko, *Geophys. Res. Lett.*, DOI: 10.1002/2015GL067316 (2016)

34. E. Priest and T. Forbes, Magnetic Reconnection: MHD theory and applications, Cambridge University Press, Cambridge (2007)

35. J.F. Drake, M. Swisdak, C. Cattell, M.A. Shay, B.N. Rogers, A. Zeiler, Science, 299, 5608 (2003)

TABLE I.

SPACECRAFT SEPARATIONS (km)

SC PAIR	PARALLEL SEPARATION	PERPENDICULAR SEPARATION
1-2	-15.4	21.7
1-3	-9.9	26.9
1-4	-29.2	9.3

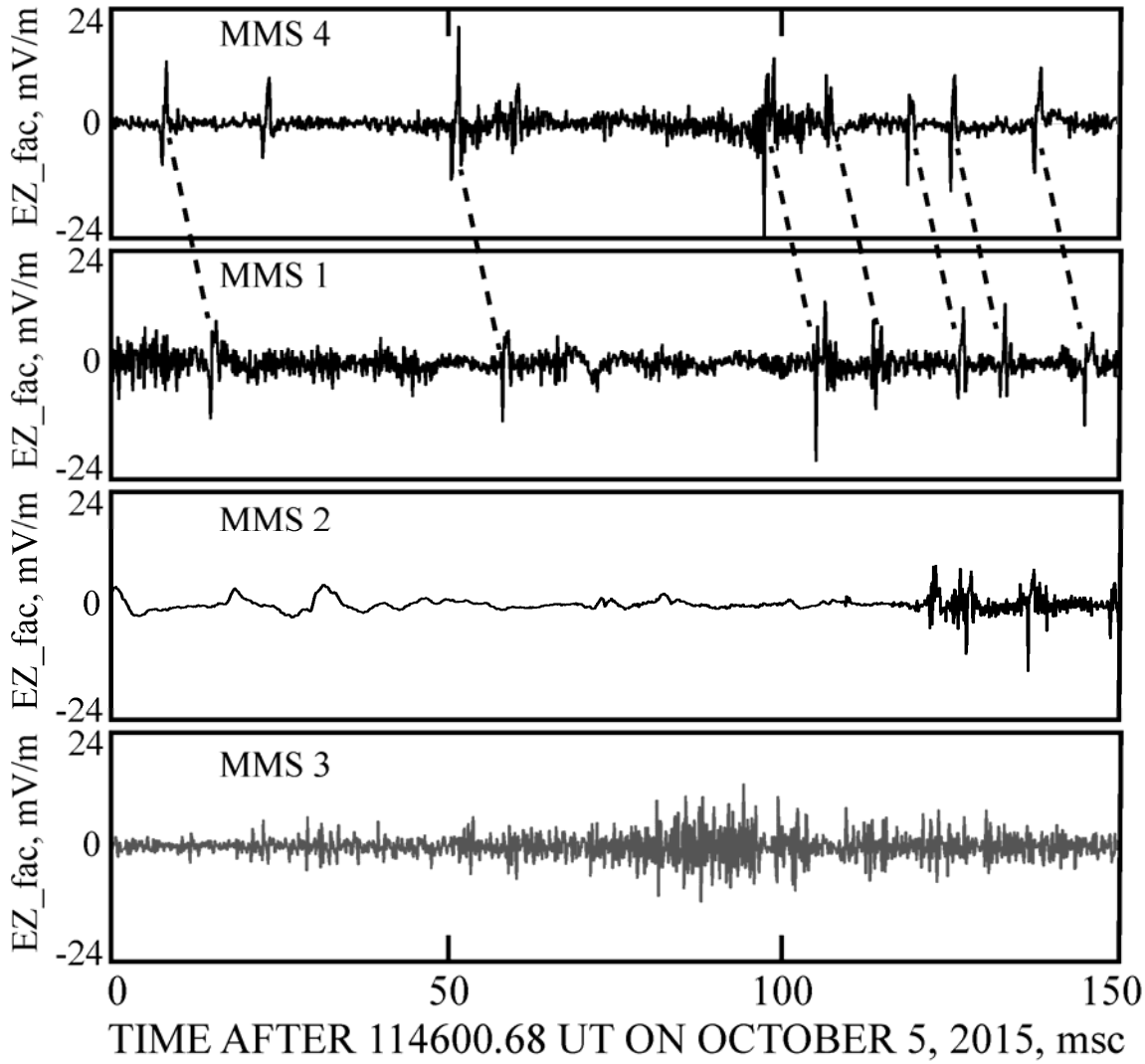

Figure 1. The electric field component parallel to the background magnetic field measured on the four MMS spacecraft during a 150 millisecond interval.

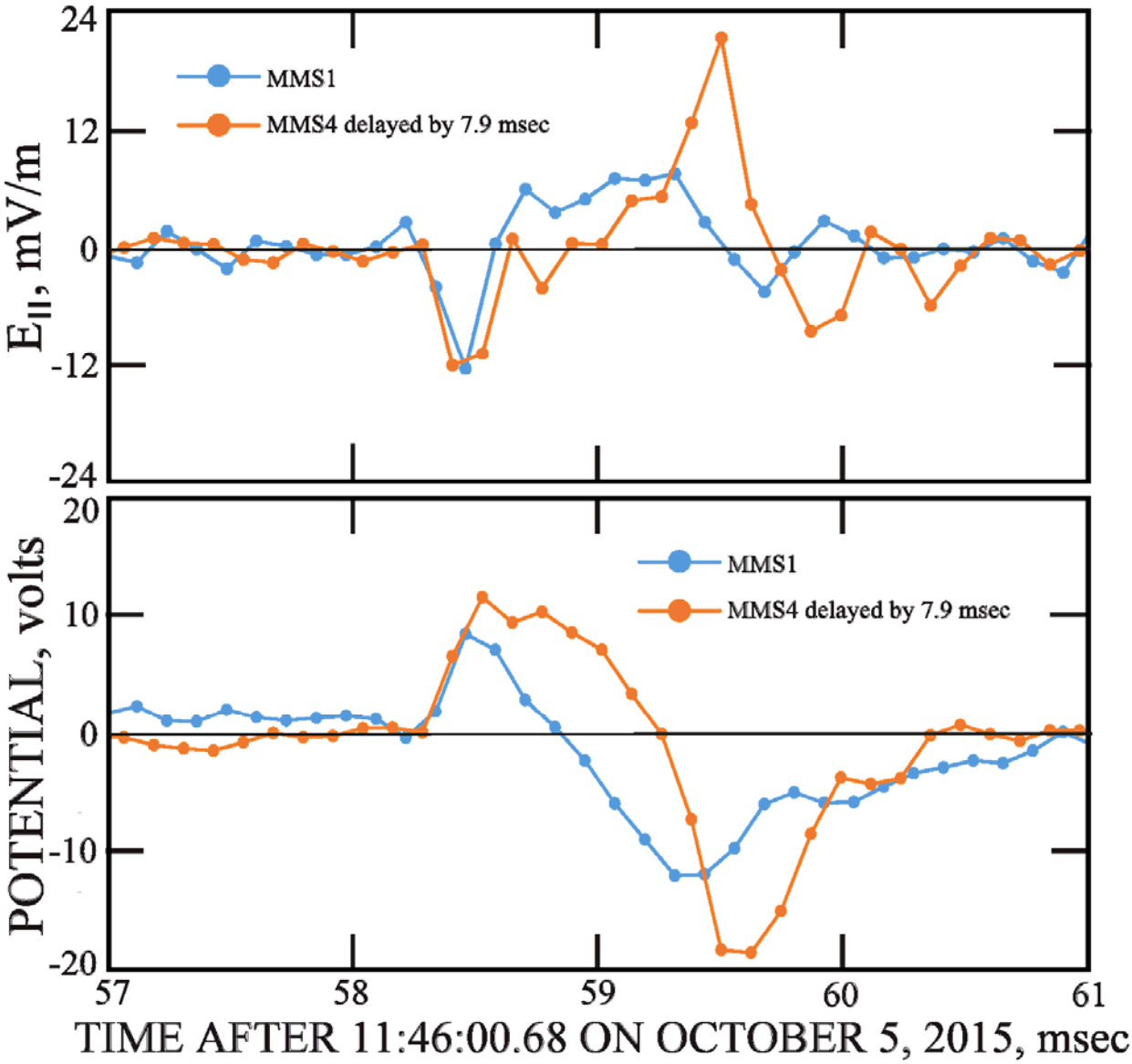

Figure 2. The electric field (top panel) and electric potential (bottom panel) associated with a single TDS that passed spacecraft MMS4 and, 7.9 milliseconds later, passed MMS1. The electric potentials of the bottom panel were obtained by integrating the electric fields of the top panel and by assuming that the distance between successive data points was the TDS speed of 4000 km/sec and the data rate was 8192 points/sec.

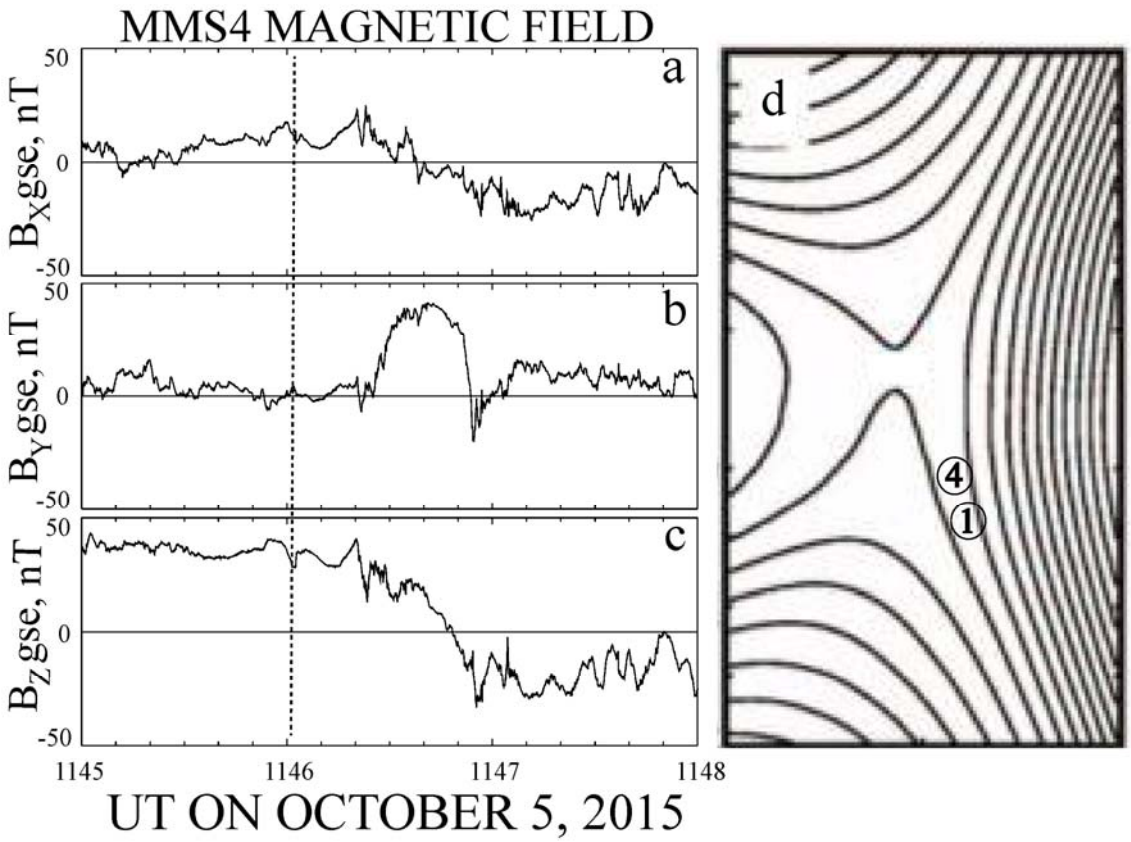

Figure 3. Panels 3a, 3b, and 3c give the three components of the magnetic field on MMS 1 at the time of the TDS (the vertical dashed line) and panel 3d illustrates the relative positions of spacecraft MMS1 and MMS4 in the reconnection geometry.

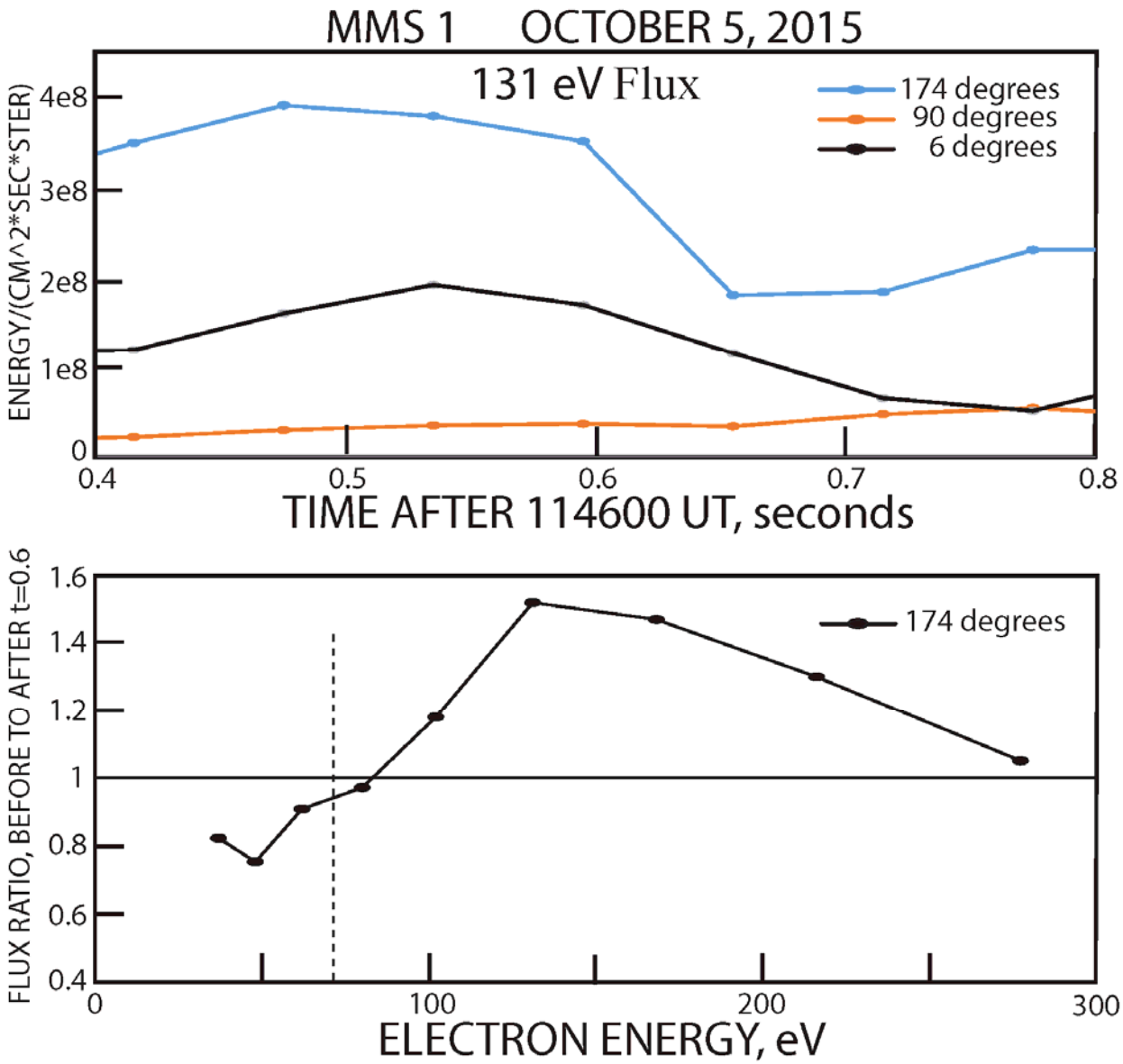

Figure 4. The upper panel gives the flux of 131 eV electrons at three pitch angles as a function of time before and after the TDS passage shortly after 0.6 seconds. The bottom panel gives the ratio of the fluxes shortly before and after the TDS as a function of energy.

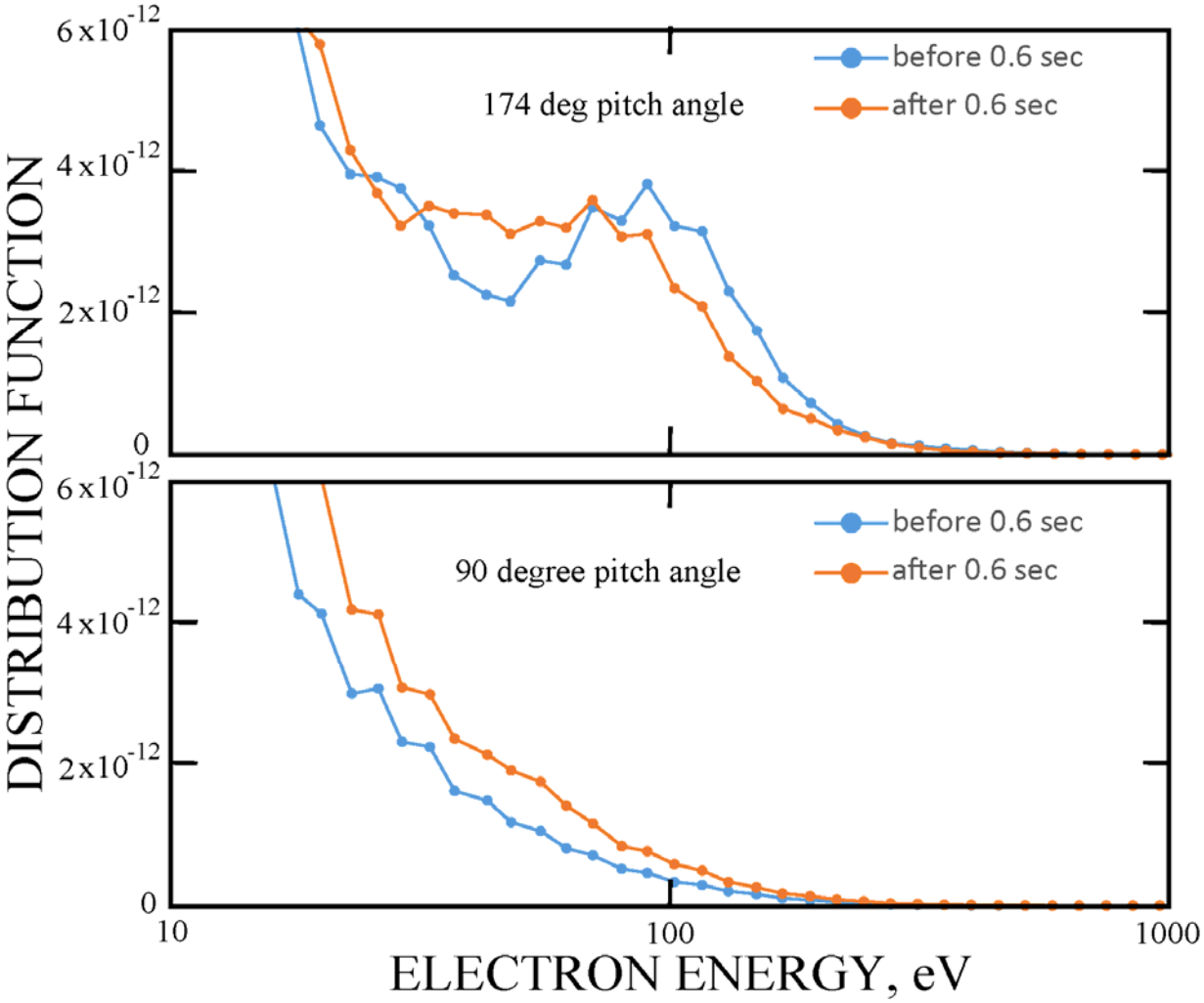

Figure 5. Distribution functions of electrons before and after TDS passage for 174 degree pitch angle electrons (top panel) and 90 degree electrons (bottom panel).

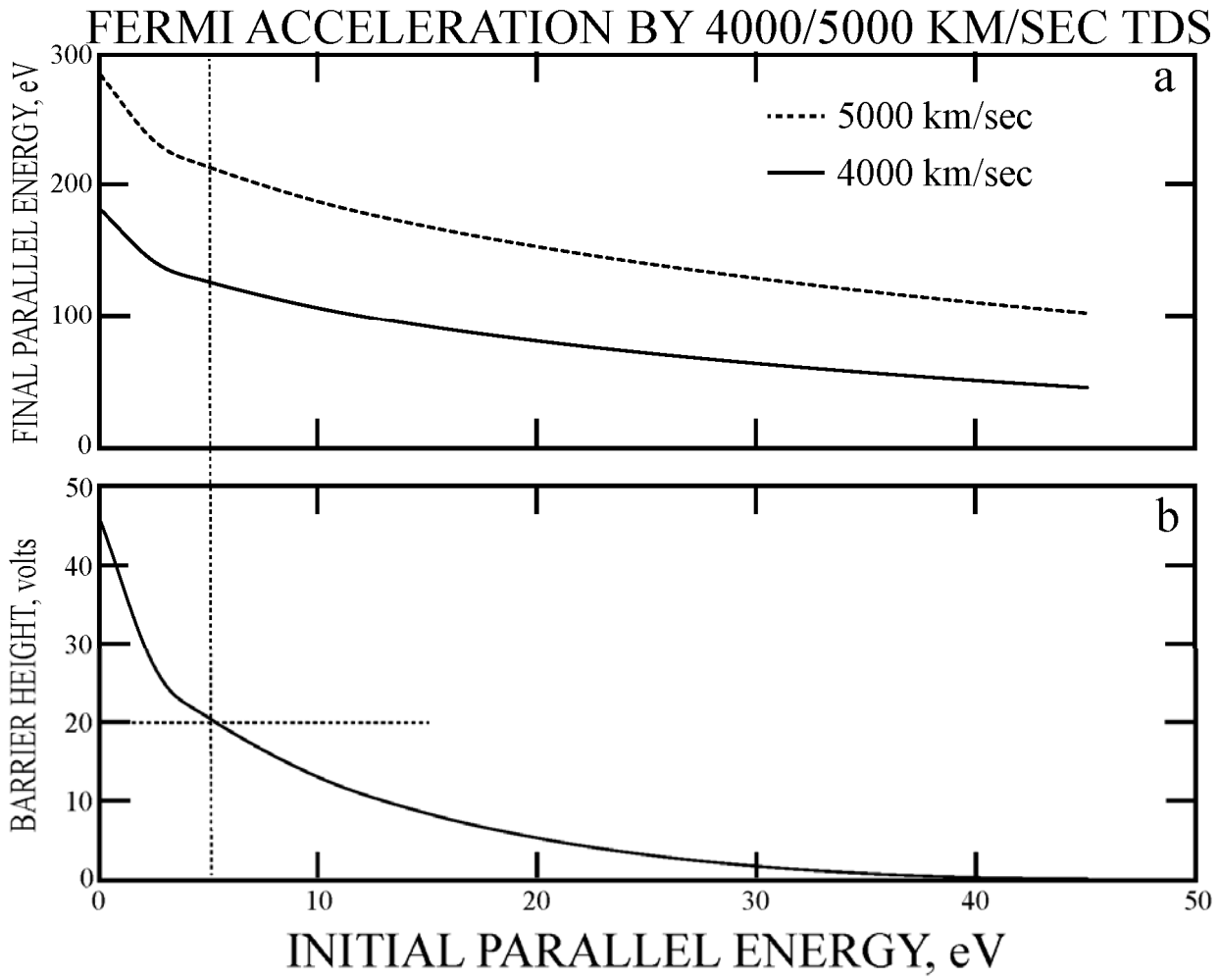

Figure 6. The top panel give the final electron energy versus its initial energy resulting from Fermi reflection of the electron by either a 4000 km/sec or 5000 km/sec TDS. The bottom panel gives the minimum initial electron energy that can be scattered by the TDS as a function of the maximum negative potential in the TDS.